Charge conservation in intact frog skeletal muscle fibres in gluconate-containing solutions

Christopher L.-H. Huang

Physiological Laboratory, Downing Street, Cambridge CB2 3EG

1. The conservation of intramembrane charge was investigated in intact voltage-clamped frog skeletal muscle fibres under conditions that minimized time-dependent ionic currents and so facilitated precise determination of capacitative charge.

2. Prolonged (q_γ) transients were demonstrated in 3,4-diaminopyridine and tetraethylammonium gluconate-containing low [Ca^{2+}] solutions in response to 125 ms pulses that explored the voltage range −90 to −20 mV. The tetracaine-sensitive, q_γ, component then accounted for a significant proportion (over 50 %) of available charge.

3. Both delayed 'on' q_γ currents and 'off' current tails decayed to steady direct current (DC) baselines without significant residual ionic current slopes in the chosen extracellular solutions. This suggested that the current transients represented capacitative decays. It was also compatible with the precise determination of effective charge by integration.

4. The advent of 'on' q_γ current was accompanied by increased 'off' charge. Thus, charge was conserved through all 'on' and 'off' steps and through test voltages that extended from the threshold appearance of q_γ as a slow transient to its full merger with the earlier q_β decay at stronger depolarizations.

5. Charge conservation persisted through a wide range of 'on' pulse durations between 60 and 370 ms and was therefore independent of the interval following the q_γ decay.

6. The quantity of q_γ charge remained a monotonic single-valued function of test voltage, whether this potential was reached directly from the −90 mV holding potential or following a prepulse to −10 mV.

7. These findings suggest that the q_γ charge movement represents the electrical signature of an intramembrane entity whose transitions are primarily driven by, and therefore conserved with, the steady-state potential.

It has frequently been assumed that charge movements in skeletal muscle represent intramembrane dipole transitions important in the regulation of physiological processes. Thus, the charge saturated beyond a defined membrane potential range and was conserved through the 'on' and 'off' portions of applied voltage steps (Schneider & Chandler, 1973; Chandler, Rakowski & Schneider, 1976). Further studies demonstrated that the overall steady-state charge was a general single-valued function of membrane potential. These findings suggested that charge movements reflected configurational changes in polar entities within the membrane primarily driven by its potential or electric field (Huang, 1983*a*).

However, charge conservation has not been tested for specific components of the intramembrane charge. For example, q_γ charge movements produce delayed transients at their most striking close to the contractile threshold (Adrian & Peres, 1979; Huang, 1981). Their steep potential dependence suggested an involvement in the intracellular Ca^{2+} release that follows tubular membrane depolarization (Irving, Maylie, Sizto & Chandler, 1989). It was initially suggested that q_γ reflects a discrete intramembrane charge (Huang, 1986, 1987; Huang & Peachey, 1989; Hui & Chandler, 1991).

However, a capacitative charge can only be determined through the integration of an unambiguously determined dielectric current component. The latter requires a full current decay to a time-invariant baseline to give the direct current (DC) membrane admittance (Adrian & Almers, 1974). However, q_γ decays were often followed by outward currents attributed to K^+ channel activation that increased over a 100 ms time scale (Adrian & Peres, 1979). There are also reports on the difficulties posed by time-dependent admittances in cut fibres (Hui & Chandler, 1991). Consequently, conservation has not been systematically examined for the q_γ charge.

The present experiments have accordingly evaluated such charge conservation. They established conditions in which q_γ charge made significant and distinguishable contributions to current records, which in turn additionally would decay fully to steady DC baselines. These requirements were accomplished using intact fibres in tetraethylammonium gluconate-containing bathing solutions (Chen & Hui, 1991)

that were further modified to minimize ionic currents. Steady-state charge displaced by voltage steps in individual unsubtracted test and control electrical records, and therefore the extent of 'on' and 'off' charge equality, could then be rigorously assessed (Adrian & Almers, 1974; Huang, 1983*a*).

METHODS

Sartorius muscles from cold-adapted frogs (*Rana temporaria*), killed by pithing and dissected in Ringer solution at 4 °C, were mounted in a temperature-controlled recording chamber. Each muscle was stretched to give fibres with a centre sarcomere length of 2·2–2·4 μm as measured using an eyepiece graticule with a Zeiss oberkochen ×40 water immersion objective (Huang & Peachey, 1989). The bathing solution was then altered first to an isotonic tetraethylammonium-containing solution, and then to a hypertonic solution after 10 min (see below). All solutions were cooled to 4–6 °C before use. The electrophysiological studies themselves followed further cooling to 2–4 °C.

The pelvic ends of superficial muscle fibres directly accessible to the bathing solution were subjected to a three-microelectrode voltage clamp (Adrian & Almers, 1976; Adrian, 1978) using conventional (4–6 MΩ) glass microelectrodes. The voltage-recording electrodes contained 3 M KCl, and the current injection electrode, 2 M potassium citrate. They were positioned at distances of $l = 375$ μm (voltage control electrode, V_1), $2l = 750$ μm (second voltage electrode, V_2) and $5l/2 = 940$ μm (current injection electrode, I_0) respectively from the fibre origin in most experiments. The distance l was reduced to 250 μm in the experiments which imposed larger voltage steps between −90 and −10 mV.

Linear fibre cable constants were determined from steady values of $V_1(t)$, $V_2(t)$ and the injected current, $I_0(t)$, at the end of depolarizing control steps made to the −90 mV holding potential. Steady levels were attained well before the terminations of the steps under present conditions. The sloping baseline corrections applied to both control and test responses in some cut fibre preparations (Melzer, Schneider, Simon & Szucs, 1986) and to test responses in intact preparations were therefore not required (Adrian & Peres, 1979). The analysis provided length constants, internal longitudinal resistances (r_i), and membrane resistances of unit fibre length (r_m). Fibre diameters (d) and specific membrane resistances (R_m) were then calculated assuming an internal sarcoplasmic resistivity (R_i) of 391 Ω cm in 2·5 times hypertonic solution at 2 °C, with a temperature coefficient (Q_{10}) of 0·73 (Hodgkin & Nakajima, 1972). The membrane current through a unit area of fibre surface, $I_m(t)$, was computed using the equation:

$$I_m(t) = [V_1(t) - V_2(t)]\, d/(6l^2 R_i),$$

where t is time. The use of intact fibres thus permitted a full cable analysis not available in cut fibre preparations, in which shunt currents beneath the Vaseline seals left r_m and therefore R_m values uncertain (Irving, Maylie, Sizto & Chandler, 1987; Chandler & Hui, 1990).

The pulse procedures investigated charge conservation through test voltages where q_γ charge contributed significantly to electrical records. They included controls for cable constant and DC current stability, the integration procedures and for the 'on' time interval.

First, control protocols interposed regularly between runs of test pulses superimposed positive, 30 or 40 mV, steps, 500 ms following negative conditioning deflections of the same magnitude. Most of the experiments varied test voltage but held pulse duration constant at 124 ms. Control averages then bracketed every set of five test runs. Experiments that varied the test pulse duration instead imposed additional control pulses of equal length before each set of test pulses. There remained bracketing by additional test and control pulses with the standard 124 ms duration to maintain consistent monitoring of fibre condition and stability. Charge movements were obtained from the difference between test records and corresponding control records scaled appropriately to the ratio of the test and control voltage excursions.

Second, successive control traces with computed cable constants were followed through each experiment (cf. Huang, 1990, 1991) to exclude drifts in fibre condition, a precaution not fully possible in cut fibres. The figure legends list the linear cable constants from control sweeps that preceded and followed the experimental runs. Third, the complete decay of both test and control currents to stable DC levels without significant time-dependent ionic currents was verified as required for clear-cut determinations of capacitative charge. Fourth, averaged time courses of test and control voltage steps, V_1, were also recorded. Comparisons of these validated charge movement determinations from the corresponding currents.

Finally, when computing the capacitative charge, Q, individual (unsubtracted) test and control records were integrated after subtraction of a template obtained by scaling the recorded (test or control) voltage step by the ratio between the DC admittance current and the voltage excursion. This precaution minimized ambiguities in the leak admittance contributions caused by variations between the waveforms of the test and control voltage clamp steps. These uncertainties would affect integration procedures applied to difference rather than individual test and control traces. Simpson's rule was applied to 'on' and 'off' transients separately (Adrian & Almers, 1974; Chandler *et al.* 1976; Adrian, 1978):

$$Q = \int [I_m(t) - (1/R_m)\Delta V_1(t)]\, dt.$$

The running integrals and their monotonic relaxation to a steady level were monitored against time (Adrian & Almers, 1974) and the net (non-linear) charge movement was deduced from a comparison of test and control integration records.

The above numerical procedures were performed on digital records of $V_1(t)$, $V_1(t) - V_2(t)$ and $I_0(t)$ obtained at a 12 bit analog-to-digital conversion interval of 200 μs. The signals were filtered through 3-pole Butterworth filters set at a cut-off frequency of 1 kHz and then sampled using a PDP 11/23 computer (Digital Equipment Corporation, Maynard, MA, USA) with a model 502 interface (Cambridge Electronic Design, Cambridge, UK). Five sweeps were averaged in each test or control record when measuring steady-state charge.

Studies were made at 2–4 °C in a modification of an extracellular solution adopted by Chen & Hui (1991). Inorganic electrolytes were obtained from British Drug Houses (BDH; Poole, Dorset; Analar grade). The basic experimental solution, buffered to pH 7, consisted of 120 mM tetraethylammonium gluconate, 2 mM $MgCl_2$, 2·5 mM RbCl, 800 μM $CaCl_2$, 1 mM 3,4-diaminopyridine, 2×10^{-7} M tetrodotoxin (both from Sigma Chemical Co., Poole, Dorset), and 3 mM *N*-2-hydroxyethylpiperazine-*N*′-2-ethanesulphonic acid (Hepes; Sigma). Tetraethylammonium gluconate was prepared by titrating 40 % tetraethylammonium hydroxide solution (Aldridge Chemical

Co., Poole, Dorset) against (50 % w/w) aqueous D-gluconic acid (Sigma) to neutrality using a Dow-Corning (UK) pH meter. The resulting stock solution was filtered through activated carbon before use. Sucrose (500 mM; Analar; BDH) was further added to make up hypertonic solutions. All experiments were performed within 1·5 h of introducing these external solutions.

RESULTS

Charge–voltage relationships in gluconate-containing solutions

Figure 1 illustrates typical results from voltage-clamped intact muscle fibres in the modified gluconate-containing hypertonic solutions. In addition, Ca^{2+} was largely replaced by Mg^{2+}, and 3,4-diaminopyridine added to the experimental solutions. These manoeuvres were expected to suppress Ca^{2+} and K^+ currents and thereby reduced errors in the determination of non-linear charge that originated from such time-dependent ionic currents.

Figure 1 (*A* and *B*) displays charge movements elicited by positive test pulses of varying amplitude made from a −90 mV holding potential. Intact fibres in gluconate showed normal charge movements qualitatively similar to currents obtained in sulphate. They displayed exponential q_β decays over most of the voltage range (Fig. 1*A*). Additional delayed q_γ components appeared at and beyond a test voltage of −47 mV even at the low gains employed to display the entire charge movement. Figure 1*B* shows transients from similar pulse protocols in the presence of 2 mM tetracaine, a means of q_β and q_γ charge separation previously validated against a wide range of other independent kinetic and steady-state criteria (Adrian & Peres, 1979; Huang, 1981, 1991; Hui, 1983*a*, *b*; Hui & Chandler, 1990; Hui & Chen, 1992*a*). There was little change in the initial amplitudes of the recorded decays, but currents were noticeably reduced at later times, consistent with selective changes in q_γ charge (Huang, 1981; Vergara & Caputo, 1982; Hui, 1983*a*).

The corresponding charge–voltage curves indicated significant contributions from both q_β (tetracaine resistant) and q_γ (tetracaine sensitive) components in gluconate. Figure 1*C* indicates that large voltage steps between −90 and −10 mV moved a total charge of 20·1 ± 2·2 nC μF^{-1}

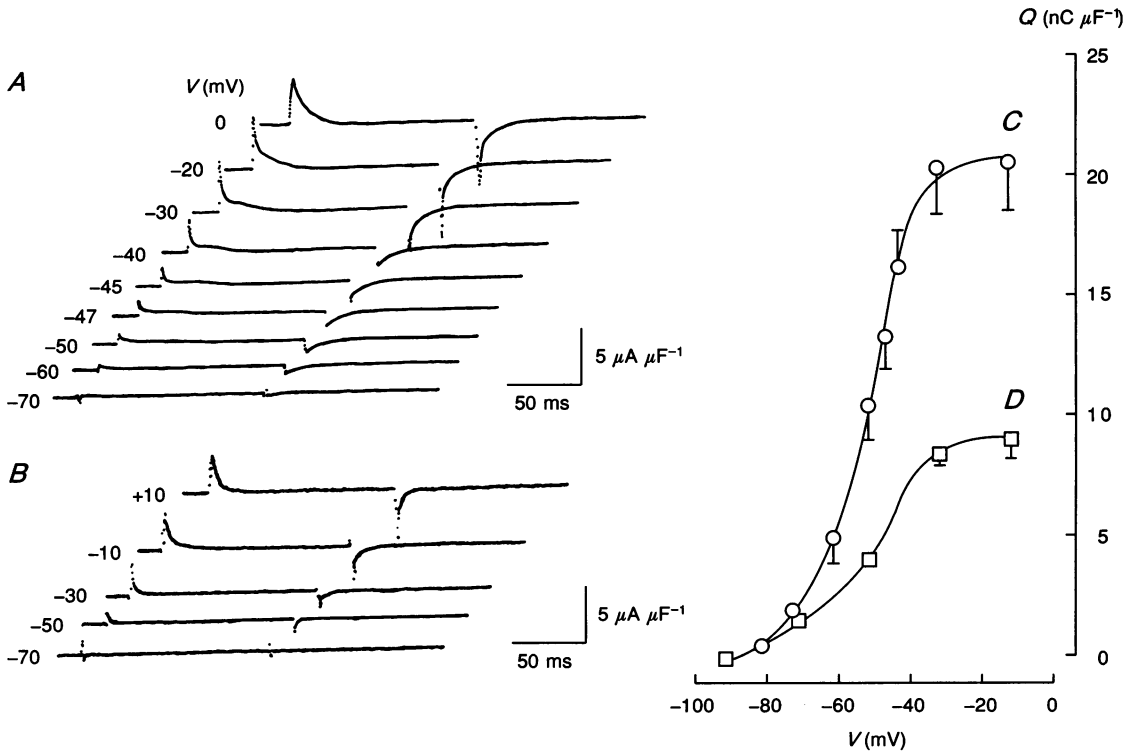

Figure 1.
Intramembrane charge movements (*A* and *B*) and the corresponding charge–voltage relationships (*C* and *D*) from fibres studied in tetraethylammonium gluconate and 3,4-diaminopyridine-containing solutions in the absence (*A* and *C*; ○: means ± S.E.M.) and the presence (*B* and *D*; □) of 2 mM tetracaine. Eight fibres studied in the absence of tetracaine: electrode spacing $l = 375\ \mu m$, temperature = 3·7 ± 0·08 °C, $R_i = 375 \pm 0{\cdot}9\ \Omega$ cm, length constant = 2·13 ± 0·21 mm, $r_i = 9968 \pm 1399\ k\Omega\ cm^{-1}$, diameter = 73·22 ± 4·93 μm, $r_m = 448{\cdot}8 \pm 82{\cdot}77\ k\Omega$ cm, $R_m = 9{\cdot}97 \pm 1{\cdot}72\ k\Omega\ cm^2$, $C_m = 7{\cdot}82 \pm 0{\cdot}68\ \mu F\ cm^{-2}$. Six fibres studied in the presence of 2 mM tetracaine: electrode spacing $l = 375\ \mu m$, temperature = 3·9 ± 0·04 °C, $R_i = 371{\cdot}9 \pm 0{\cdot}45\ \Omega$ cm, length constant = 1·84 ± 0·21 mm, $r_i = 9725 \pm 1808\ k\Omega\ cm^{-1}$, diameter = 76·2 ± 7·71 μm, $r_m = 304{\cdot}4 \pm 59{\cdot}5\ k\Omega$ cm, $R_m = 6{\cdot}9 \pm 1{\cdot}25\ k\Omega\ cm^2$, $C_m = 7{\cdot}0 \pm 0{\cdot}73\ \mu F\ cm^{-2}$.

(mean ± standard error of the mean (S.E.M.); $n = 8$ fibres). Figure 1*D* displays charge–voltage data in six fibres studied within 1 h of the addition of 2 mM tetracaine and isolated a maximum q_β charge of 9·0 ± 0·82 nC μF^{-1}. Gluconate thus reduced the maximum charge compared to earlier values from intact or cut preparations in sulphate or chloride-containing solutions (28–30 nC μF^{-1}) with a preferential reduction of q_β charge (from 15 to 20 nC μF^{-1}: Huang, 1982;

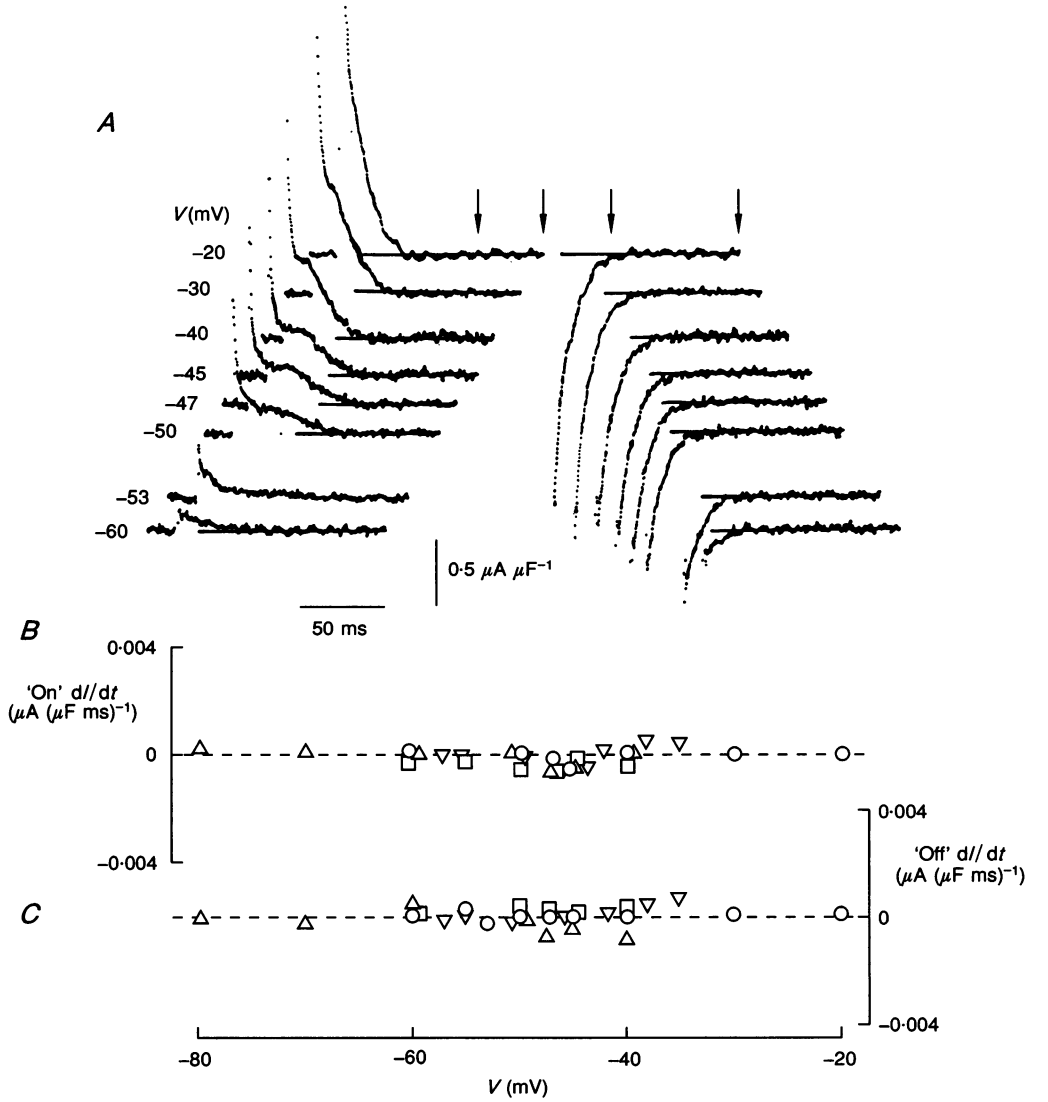

Figure 2. Intramembrane charge movements displayed at a high gain in order to demonstrate delayed q_γ charge movements in gluconate-containing solutions

A, examination of baseline slopes following 'on' (left) and 'off' (right) decays in charge movements explored through voltages of −60 and −20 mV in close increments, at voltages at which there were decays of delayed (q_γ) charge. Fibre V17: electrode spacing $l = 375$ μm, temperature = 3·8 °C, $R_i = 373{\cdot}5$ Ω cm, diameter = 79·97 μm. Fibre cable constants prior to test runs: length constant = 1·75 mm, $r_i = 7435$ kΩ cm^{-1}, $r_m = 227{\cdot}3$ kΩ cm, $R_m = 5{\cdot}71$ kΩ cm^2, $C_m = 5{\cdot}52$ μF cm^{-2}. Cable constants following test runs: length constant = 1·85 mm, $r_i = 8296$ kΩ cm^{-1}, $r_m = 284{\cdot}7$ kΩ cm, $R_m = 6{\cdot}77$ kΩ cm^2, $C_m = 5{\cdot}92$ μF cm^{-2}. *B* and *C*, results of least-squares fits to obtain slopes of the last 40 ms of the 'on' decays (*B*) and the last 80 ms of the 'off' decays (*C*) in four fibres identified in Fig. 3. Four fibres: electrode spacing $l = 375$ μm, temperature = 3·85 ± 0·08 °C, $R_i = 371{\cdot}4 \pm 0{\cdot}61$ Ω cm, diameter = 75·7 ± 8·2 μm. Fibre cable constants before test runs: length constant = 1·77 ± 0·22 mm, $r_i = 9967{\cdot}7 \pm 2875{\cdot}1$ kΩ cm^{-1}, $r_m = 261{\cdot}8 \pm 26{\cdot}05$ kΩ cm, $R_m = 6{\cdot}19 \pm 0{\cdot}96$ kΩ cm^2, $C_m = 6{\cdot}63 \pm 0{\cdot}76$ μF cm^{-2}. Fibre cable constants following experimental runs: length constant = 1·71 ± 0·24 mm, $r_i = 12467{\cdot}9 \pm 4541{\cdot}8$ kΩ cm^{-1}, $r_m = 272{\cdot}3 \pm 21{\cdot}65$ kΩ cm, $R_m = 6{\cdot}13 \pm 1{\cdot}02$ kΩ cm^2, $C_m = 7{\cdot}09 \pm 0{\cdot}65$ μF cm^{-2}.

Hui, 1983*a*; Hui & Chandler, 1990). This confirms recent findings in which the replacement of chloride by gluconate suppressed q_β charge by 75 % but q_γ charge by only 22 % in cut fibres (Chen & Hui, 1991).

Finally, comparisons of the two charge–voltage curves (Fig. 1*C* and *D*) also suggested a negative, 5–10 mV, shift in the voltage dependence of the q_γ (tetracaine susceptible) component in gluconate. Consequently, there was a small, but nevertheless appreciable, q_γ charge movement, even at a test potential of −60 mV, in contrast to the usual q_γ threshold close to −45 mV in sulphate-containing solutions (Huang, 1982).

These changes together meant that the q_γ component accounted for an increased proportion of the total charge movement over the test voltage range through which its delayed transients were discernible in charging records. Thus, the total charge was $10{\cdot}6 \pm 1{\cdot}57$ and $20{\cdot}58 \pm 2{\cdot}11$ nC μF^{-1} (mean ± S.E.M.; $n = 8$ fibres) at test voltages of −50 and −30 mV respectively. In contrast, the corresponding amount of q_β or tetracaine-resistant charge was $4{\cdot}1 \pm 0{\cdot}19$ and $8{\cdot}56 \pm 0{\cdot}57$ nC μF^{-1} respectively ($n = 6$ fibres). Hence, the q_γ component made up over 50 % of the total charge movement in this voltage range. The present conditions therefore enhanced the discrimination of q_γ currents from the overall charge movement.

Delayed (q_γ) charge movements are prominent in gluconate-containing solutions

Figure 2*A* displays q_γ charge movements at high magnification in intact fibres in gluconate-containing solutions. The test voltage steps were closely incremented to between −60 mV, a value subthreshold to slow q_γ charge movements, and −20 mV, at which q_γ currents had merged with and become indistinguishable from the earlier q_β decays. The test steps were made from a fixed −90 mV holding potential and were bracketed by control steps as detailed in the Methods. A comparison of the first and last of the latter control records yielded flat difference traces, confirming fibre stability throughout the procedure.

Delayed (q_γ) 'on' currents appeared from a test voltage of −50 mV. They were prolonged over 50 ms between potentials of −50 and −47 mV. 'Off' currents could be compared at voltages subthreshold (at −53 and −60 mV in Fig. 2A) and just suprathreshold (at −50 and −47 mV) to the delayed currents. This indicated that the onset of 'on' q_γ currents was associated with increased amplitudes in the 'off' tails.

The q_γ transients varied steeply with test voltage, becoming substantially more rapid with even a little (less than 10 mV) further depolarization. Nevertheless, early (q_β) and delayed (q_γ) currents could be distinguished over a wide voltage range of between −50 and −30 mV in the present solutions, despite the use of large rather than small (10 mV) testing steps (Adrian & Peres, 1979; Huang 1981, 1982). Thus the shifted voltage dependence of q_γ currents, together with the selective reduction of q_β currents accomplished here, optimized scrutiny of the q_γ charge.

The q_γ currents decay to steady (DC) baselines in gluconate-containing solutions

Figures 2–4 illustrate findings from systematic investigations into charge conservation and the necessary conditions for its assessment in four muscle fibres. Fibres were studied through pulse procedures particularly associated with delayed 'on' q_γ charge movements. Figures 2 and 3 display both records obtained from one typical fibre (*A*) and individual results from the entire data set (*B*). The extent of both 'on' and 'off' current decay that followed the capacity transient was first explored to establish an unambiguous determination of the DC current component. Figure 2*A* plots charge movements at high gain to emphasize both q_γ decays and the DC baselines, with 'on' and 'off' responses shown separately for clarity. The superimposed lines show least-squares fits that determined the linear slopes of the last 40 ms of the 'on' currents and of the last 80 ms of the 'off' currents respectively. A fitting procedure to the last 60 ms of both 'on' and 'off' currents instead gave similar slopes. These procedures were not applied to decays whose time courses approached the actual record length (see also Hui & Chandler, 1991) as occurred with the 'on' record at the −53 mV test voltage (Fig. 2*A*).

Consistent use of the above criteria for the final current baseline suggested complete decays of both 'on' and 'off' membrane currents to steady DC levels even in the presence of delayed 'on' q_γ currents (Fig. 2*A*). Significant dips in the charging currents below the baseline could not be demonstrated against the baseline noise. In the intact fibres studied here, 'off' decays were relatively rapid and did not show the prolonged tails demonstrated in cut fibres at some voltages (Hui & Chandler, 1991) or in intact fibres in the presence of perchlorate (Huang, 1987). The plots of 'on' (Fig. 2*B*) and 'off' (Fig. 2*C*) final current slopes for four fibres showed small absolute magnitudes everywhere less than $0{\cdot}0007$ μA (μF ms)$^{-1}$. The values were independent of test potential. There were no departures from the overall horizontal straight line relationship, either with onset of prolonged q_γ transients or with their merger with the q_β decays at more positive test potentials. This complete and consistent decay to a steady DC baseline is consistent with dielectric relaxation processes (Schneider & Chandler, 1973; Chandler *et al.* 1976; Huang, 1981, 1983*a*, *b*).

Charge is conserved with the appearance of the q_γ component

The flat regression lines indicated above accordingly gave DC pedestals suitable for determinations of steady-state charge from the current records. Figure 3 compares the corresponding 'on' and 'off' charges through test voltages clustered about the q_γ threshold but which also extended to more positive potentials that merged the q_β and q_γ currents. Integration of the prolonged test trace at −53 mV assumed the baseline obtained from the record of −50 mV: this would overestimate rather than underestimate 'on' charge. First, the running integrals of the charge movements

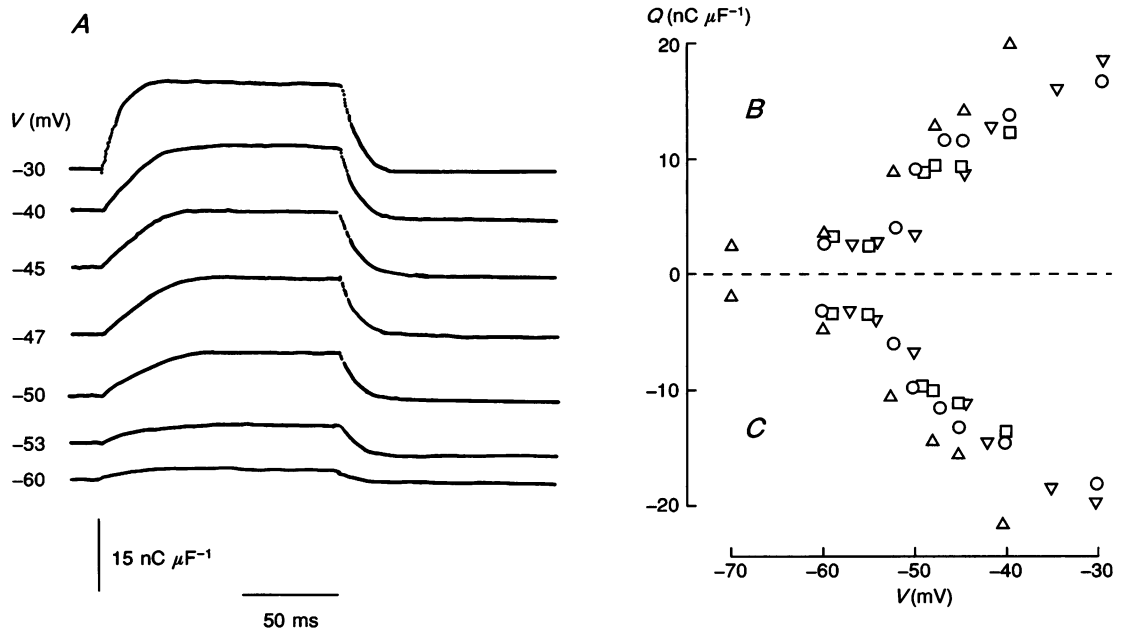

Figure 3.
A, running integrals of non-linear transient currents at different test voltages, derived from running integrals of test and scaled control transients, through the voltages at which delayed q_γ currents could be discerned in charging records. Traces are from the same fibre, V17, as described in the legend to Fig. 2. *B* and *C*, comparisons of 'on' (*B*) and 'off' (*C*) charge from the four fibres described in the legend to Fig. 2. ○, fibre V17; △, V18; □, V20; ▽, V21.

through the 'on' and 'off' steps, derived from separate integrations of control and test records, confirmed that charge increased monotonically with time to a steady value. Second, there was a zero net charge movement with the end of the 'off' steps (Fig. 3*A*). Third, both 'on' (Fig. 3*B*) and 'off' (Fig. 3*C*) steady-state charge increased smoothly with depolarization from the holding voltage in each fibre with no evidence for any non-monotonic voltage dependence as the two kinetic components fused, contrary to earlier suggestions (p. 913 in Pizarro, Csernoch, Uribe, Rodriguez & Rios, 1991). Finally, comparisons of Fig. 3*B* and *C* confirm an 'on' and 'off' equality through the entire explored voltage range. A plot of 'on' against 'off' charge (Fig. 4) gave points close to equality and a least-squares fit through the origin (thick line) with a slope $m = 0{\cdot}959 \pm 0{\cdot}0119$ ($n = 29$ points) close to unity (Fig. 4; thin line). There were no marked deviations from this straight-line 'on'–'off' relationship either at the threshold of the q_γ 'on' currents or with larger test steps at which the q_β and q_γ waveforms fused.

'Off' charge conservation is independent of 'on' pulse interval

A further set of experiments tested charge conservation in the face of varying 'on' pulse duration (Fig. 5). A range of

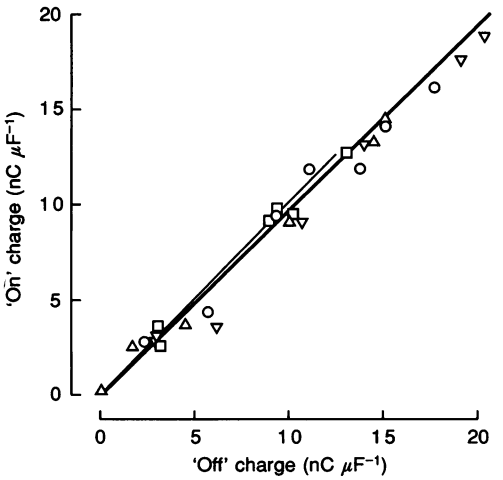

Figure 4. Plots of 'on' against 'off' charge in the depolarizing voltage range at which q_γ transitions take place
The least-squares slope of the line drawn through the origin (thick line) is $0{\cdot}959 \pm 0{\cdot}0199$. Same fibre set and symbols as in Figs 2 and 3.

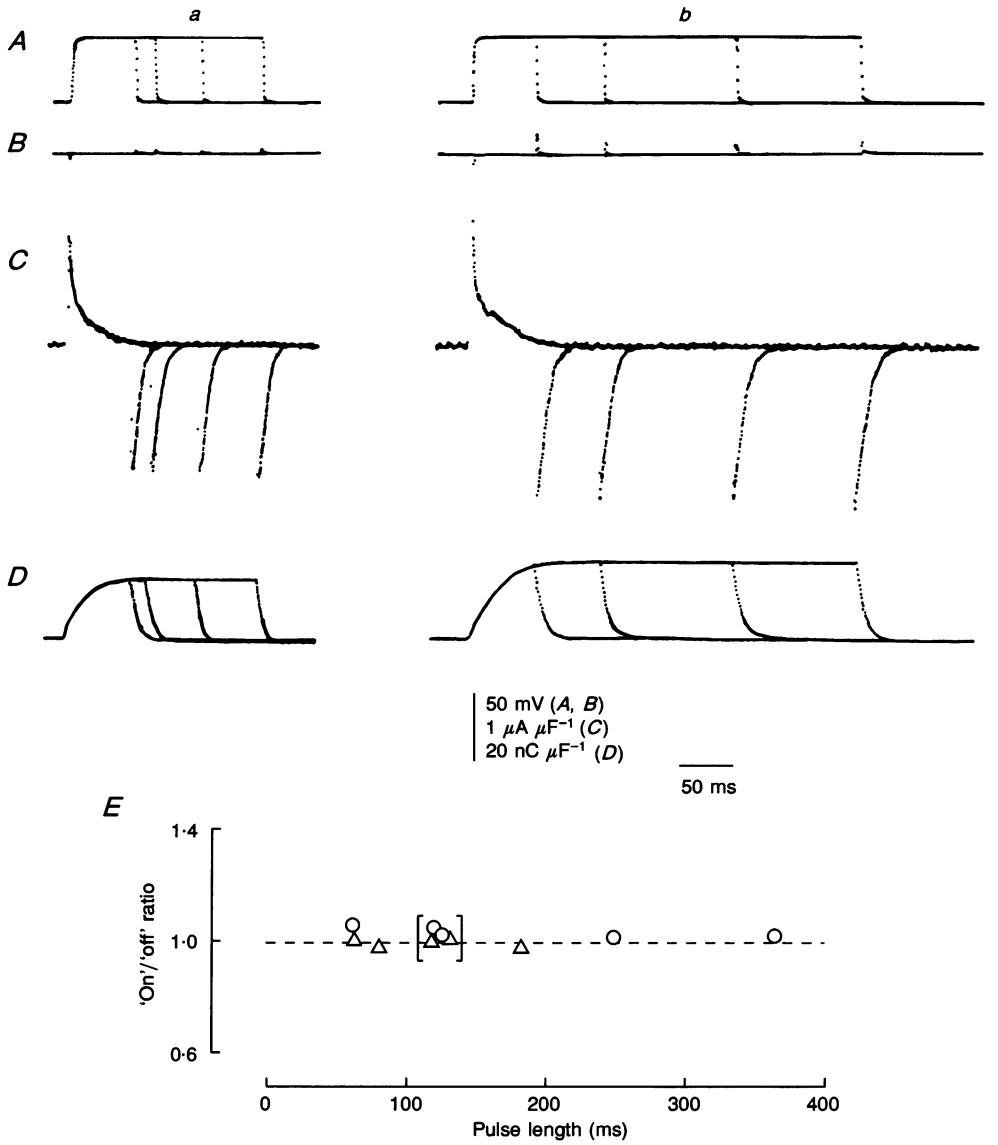

Figure 5.

Investigation of q_γ charge conservation at different 'on' pulse lengths in the overlapping ranges 62–182 ms (left traces; fibre V27) and 62–364 ms (right traces; fibre V21). These demonstrate test voltage waveforms to level $V = -40$ mV for the pair of fibres displayed here (*A*), the difference between test and scaled control voltage waveforms (*B*), the resulting charge movements (*C*), their running integrals (*D*) and 'on'/'off' charge ratios plotted against pulse length for fibre V27 (△) and fibre V21 (○) (*E*). The pairs of points in square brackets in (*E*) denote the ratios obtained in runs that adopted a control pulse length of 124 ms and which were performed respectively at the beginning and the end of each run. Fibre V27 was studied through the range of short pulse lengths: mean 'on' charge movement through the voltage steps at the adopted test voltage = 17·9 ± 0·37 nC μF^{-1}; electrode spacing $l = 375$ μm, temperature = 3·5 °C, $R_i = 416{\cdot}7$ Ω cm, diameter = 44·6 μm. Fibre cable constants prior to test procedures: length constant = 1·034 mm, $r_l = 27750$ kΩ cm^{-1}, $r_m = 298{\cdot}2$ kΩ cm, $R_m = 4{\cdot}09$ kΩ cm^2, $C_m = 4{\cdot}06$ μF cm^{-2}. Cable constants following test runs: length constant = 1·11 mm, $r_l = 26075$ kΩ cm^{-1}, $r_m = 321{\cdot}6$ kΩ cm, $R_m = 4{\cdot}56$ kΩ cm^2, $C_m = 4{\cdot}38$ μF cm^{-2}. Fibre V21 studied at the longer pulse lengths: mean 'on' charge at adopted test potential = 23·4 ± 0·74 nC μF^{-1}; electrode spacing $l = 375$ μm, temperature = 3·6 °C, $R_i = 369{\cdot}9$ Ω cm, diameter = 48·7 μm. Fibre cable constants prior to test runs: length constant = 1·22 mm, $r_l = 19836$ kΩ cm^{-1}, $r_m = 298{\cdot}2$ kΩ cm, $R_m = 4{\cdot}56$ kΩ cm^2, $C_m = 4{\cdot}81$ μF cm^{-2}. Cable constants following test runs: length constant = 1·0 mm, $r_l = 28132{\cdot}1$ kΩ cm^{-1}, $r_m = 277{\cdot}8$ kΩ cm, $R_m = 3{\cdot}57$ kΩ cm^2, $C_m = 5{\cdot}14$ μF cm^{-2}.

exploratory test steps made from a fixed, −90 mV, holding potential first ascertained a voltage level V' which elicited q_γ currents as distinguishable delayed waveforms. The subsequent test voltage steps then adopted a more depolarized fixed level V at which the q_γ decays became more rapid and so left longer DC baselines more amenable to the integration procedures; thus, $V = (V' + 5)$ mV. These test steps imposed either (a) a series of short, but closely incremented test pulse lengths in the range 62–182 ms, or (b) a range of longer pulse lengths between 62 and 364 ms, which nevertheless partly overlapped the intervals used in (a) (Fig. 5*A a* and *b*).

Comparison of the test voltage records (Fig. 5*A*) with their appropriately scaled corresponding controls of the same length gave subtraction traces close to zero (Fig. 5*B*). Similar scaled subtractions of test and control current traces therefore yielded legitimate representations of the charge movement. The latter records (Fig. 5*C*) showed superimposable 'on' transients and that all the 'off' steps began after the full decay of even the delayed 'on' q_γ currents. Neither the initial magnitude nor the subsequent form of the 'off' currents, then, were influenced by 'on' pulse duration. Similarly, all the corresponding 'on' integration records were superimposable and fully returned to net zero charge movement with recovery from the 'off' steps (Fig. 5*D*). Finally, all 'on'/'off' ratios for non-linear charge were close to unity (Fig. 5*E*; dotted line), and to bracketing values obtained from 124 ms-long pulses (Fig. 5*E*; symbols in square brackets).

This persistence of charge conservation despite wide (62–364 ms) variations in pulse length strongly suggests that the 'off' charge movement reflects transitions driven primarily by membrane potential.

Charge movement is conserved through sets of additive voltage steps

Figures 6 and 7 illustrate further, more general tests for charge conservation at a test voltage V reached through different paths. The latter involved the potential range between −90 and −10 mV, through which the q_γ system is voltage dependent in the steady state (Fig. 1*C* and *D*). Similar tests have been applied to q_β charge on earlier occasions (Huang, 1983*a*).

A series of exploratory test steps first ascertained a voltage V' which would trigger slow 'on' q_γ charge movements. It was then possible to set a test level V at which there would be appreciable q_γ charge movement; thus, $V = (V' + 5)$ mV (Fig. 7*A*). A cycle of test pulses then compared the charge Q when the voltage V was reached directly from the −90 mV holding potential with the net charge when V was reached following prior charge saturation by a prepulse step to −10 mV. This also simultaneously

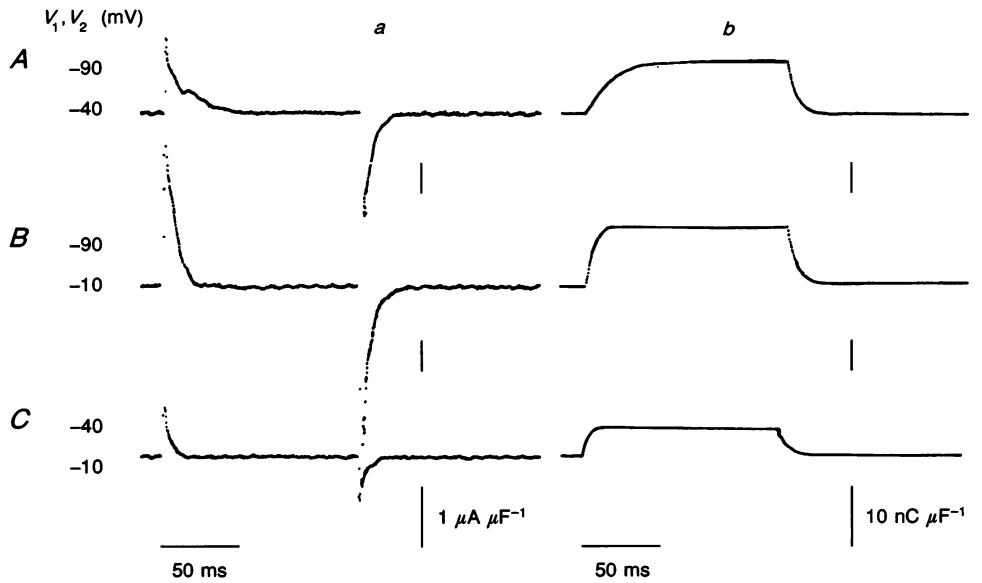

Figure 6.
Comparisons of charge movements (*a*) and running integrals (*b*) elicited by voltage steps between a fully polarized membrane potential of −90 mV and a test level of −40 mV (*A*), a fully polarized membrane potential of −90 mV and a test level of −10 mV (*B*), and a prepulse voltage of −40 mV and a test voltage of −10 mV (*C*). The last step (*C*) was imposed 500 ms following introduction of the prepulse step. Pulse duration 124 ms. Fibre V37: electrode spacing $l = 250$ μm, temperature = 3·6 °C, $R_i = 389$ Ω cm, diameter = 46·7 μm. Fibre cable constants prior to test runs: length constant = 1·01 mm, $r_i = 22738$ kΩ cm^{-1}, $r_m = 221{\cdot}6$ kΩ cm, $R_m = 3{\cdot}25$ kΩ cm^2, $C_m = 5{\cdot}07$ μF cm^{-2}. Cable constants following test runs: length constant = 0·93 mm, $r_i = 24429$ kΩ cm^{-1}, $r_m = 210{\cdot}6$ kΩ cm, $R_m = 2{\cdot}98$ kΩ cm^2, $C_m = 5{\cdot}03$ μF cm^{-2}.

tested for 'on'/'off' charge equality through the respective voltage excursions through the intervals (−90 mV, V), (V, −10 mV) and (−90 mV, −10 mV). Thus (a) simple test pulses were applied between −90 mV and the test level $V = -40$ mV (Figs 6*A* and 7*A*), (b) large test pulses were applied between −90 mV and the saturating level of −10 mV (Figs 6*B* and 7*B*), and (c) test pulses were imposed 500 ms following a prepulse step to V to a voltage of −10 mV (Figs 6*C* and 7*C*). Finally, all these test pulses were bracketed by control +40 mV steps superimposed on a prepulse to −130 mV. Comparison of the test and appropriately scaled control voltage records gave traces close to zero (Fig. 7*A*, *B* and *C*; lower traces).

Figure 6 shows (*a*) charge movements determined by comparing test and appropriately scaled control records and (*b*) their running integrals derived from the respective control and test voltage records following DC corrections for a typical fibre. The latter confirmed net zero charge movement through all types of test step. Figure 7 displays the corresponding 'on' (open symbols) and 'off' charges (filled symbols in each pair: means ± S.E.M.; $n = 3$ fibres). First, 'on' and 'off' charge was equal through all the test pulses (*A*–*C*) (Fig. 7). Second, the sum of the charge movement through a direct pulse from −90 mV to V (Fig. 7*A*; left ordinate) and that transferred between prepulse level V and −10 mV (Fig. 7*C*; right ordinate) equalled the charge moved by a a direct step through the same range, between −90 and −10 mV (Fig. 7*B*; left ordinate) with an overall ratio, $(B)/[(A)+(C)]$ of 0·986 ± 0·019. Hence net charge movement was additive through different combinations of voltage step.

DISCUSSION

This study evaluated charge conservation through the 'on' and 'off' parts of applied voltage steps specifically for q_γ charge (Adrian & Peres, 1979; Huang, 1981). This required leak admittance contributions to individual test and control charging records to be determined from templates derived from the waveforms of the applied voltage steps. The latter traces were scaled to steady DC levels determined *a priori* from the respective test and control current traces (see also Hui & Chandler, 1991). Only then could their dielectric contributions be determined unambiguously for integration to give the steady-state capacitative charge (Adrian & Almers, 1974). This separation was precluded in earlier

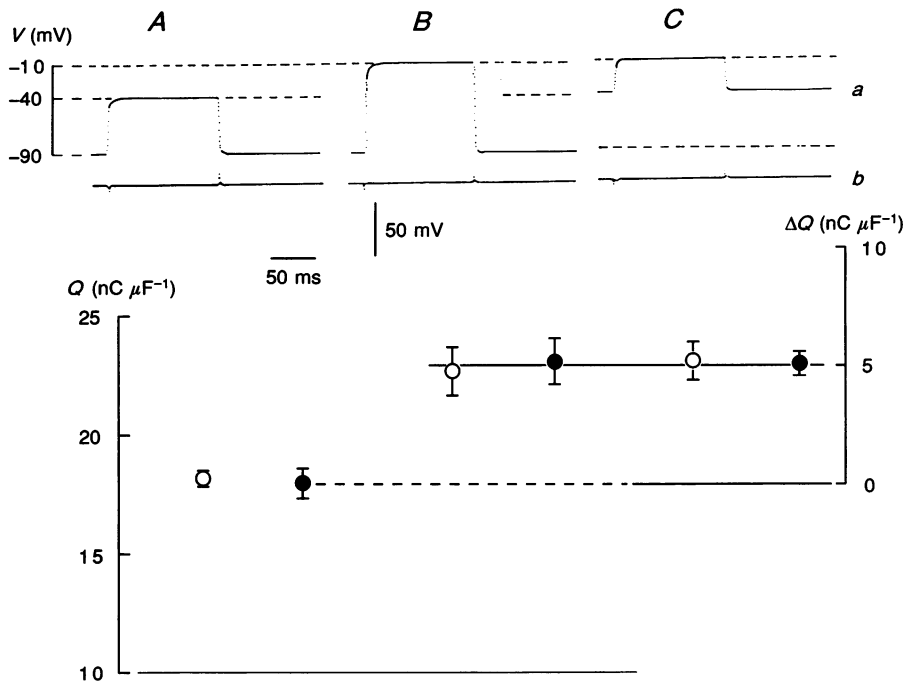

Figure 7.
Additivity of the integrated 'on' (○) and 'off' (●: means ± S.E.M.) charge obtained in response to voltage steps between a fully polarized membrane potential of −90 mV and a test level of −40 mV (*A*), a fully polarized membrane potential of −90 mV and a test level of −10 mV (left ordinate) (*B*) and a prepulse voltage of −40 mV and a test level of −10 mV (right ordinate) (*C*). The last step (*C*) was imposed 500 ms following introduction of the prepulse step. Three fibres: electrode spacing $l = 250$ μm, temperature = 3·53 ± 0·05 °C, $R_i = 396{\cdot}3 \pm 8{\cdot}9$ Ω cm, diameter = 56·1 ± 4·6 μm. Fibre cable constants before pulse cycle: length constant = 1·15 ± 0·06 mm, $r_i = 16591{\cdot}4 \pm 2511{\cdot}9$ kΩ cm^{-1}, $r_m = 209{\cdot}4 \pm 7{\cdot}48$ kΩ cm, $R_m = 3{\cdot}71 \pm 0{\cdot}19$ kΩ cm^2, $C_m = 7{\cdot}69 \pm 1{\cdot}08$ μF cm^{-2}. Fibre cable constants following the pulse cycle: length constant = 1·05 ± 0·07 mm, $r_i = 16897{\cdot}6 \pm 3391{\cdot}9$ kΩ cm^{-1}, $r_m = 175{\cdot}3 \pm 14{\cdot}7$ kΩ cm, $R_m = 3{\cdot}08 \pm 0{\cdot}09$ kΩ cm^2, $C_m = 8{\cdot}26 \pm 1{\cdot}6$ μF cm^{-2}.

studies by the slow outward currents, attributed to the delayed rectifier, that followed the q_γ decays (Adrian & Peres, 1979).

The analysis procedures also required records to which q_γ currents made substantial and distinguishable contributions. The DC baselines could then be determined in individual test and control trials rather than from difference traces. Thus, q_γ currents were not distinct in some cut fibre studies that accordingly compared currents before and after manoeuvres that inhibited q_γ charge (Csernoch, Pizarro, Uribe, Rodriguez & Rios, 1991; Garcia, Pizarro, Rios & Stefani, 1991). This approach gave biphasic difference traces in which the initial outward q_γ currents were additionally followed by inward current decays. The latter were a necessary condition for a hypothesis in which q_γ currents resulted from a membrane binding of released intracellular Ca^{2+} as this would require a reverse current following the subsequent Ca^{2+} removal from such sites. Alternatively, such effects could also result from kinetic changes in the q_γ system resulting from the interposed experimental manoeuvres (see Hui, 1991; Hui & Chen, 1992*a*, *b*; Chandler, Jong & Pape, 1992; Pape, Jong & Chandler, 1992). At all events, the ionic current templates in such difference traces would be inherently uncertain. Thus, use of the late sloping baseline would give rise to an excessive 'on' integral (Csernoch *et al.* 1991; Pizarro *et al.* 1991).

The studies here overcame these difficulties. The substitution of gluconate for sulphate preferentially reduced q_β charge and shifted the voltage dependence of q_γ charge in the negative direction. The q_γ system now contributed over 50 % of charge movement through the voltages explored. These manoeuvres also extended the potentials in which q_γ currents were discernible. Finally, intact fibre preparations gave a greater inherent baseline stability in their records than did cut fibres. Thus the control decays did not require slope corrections (Melzer *et al.* 1986; Huang & Peachey, 1989; Huang, 1990); with the extracellular electrolyte substitutions and pharmacological conditions introduced here, neither did the test currents, including records that displayed q_γ charge movements.

It was accordingly possible to achieve a quantitative determination of charge movements and so to establish the following features of the q_γ charge for the first time. First, both 'on' and 'off' q_γ currents could decay fully through wide variations in either test voltage or pulse interval (62–364 ms), without being followed by 'dips' or upward slopes. Second, 'on' and 'off' charge equality held through the entire voltage range that extended between the threshold for slow q_γ currents and their merger with the q_β decays, in contrast to earlier cut fibre reports (Szucs, Csernoch, Magyar & Kovacs, 1991). Third, both the 'on' and the 'off' charge increased with progressive depolarization without evidence for any non-monotonic dependence upon voltage (cf. p. 913 of Pizarro *et al.* 1991). Fourth, charge conservation extended to pulses that varied the 'on' interval immediately following q_γ decay. Finally, a test voltage V transferred the same net charge Q whether V was reached directly from the −90 mV holding potential or indirectly via a saturating prepulse potential of −10 mV. 'On' charge equalled 'off' charge through all the latter manoeuvres.

The q_γ component is of interest in view of its highly non-linear and steeply voltage-dependent steady-state and kinetic properties and its identification with intramembrane dihydropyridine receptors thought to be involved in excitation–contraction coupling (Huang, 1990; Huang & Peachey, 1992). The observations here provide systematic evidence for its charge conservation. They additionally require charge transfer to be additive through different combinations of voltage step. They thus suggest that q_γ currents reflect capacitative intramembrane charge redistributions driven primarily by potential. They could permit alternative driving parameters such as the membrane binding of released intracellular Ca^{2+}, as suggested by Csernoch *et al.* (1991). However, the conservation properties demonstrated here, then, would require the driving process to increase monotonically with voltage, show time invariance over the explored intervals following 'on' q_γ charge movement, and to be additive through combinations of voltage steps. Nevertheless such predictions may merit further experimental testing.

REFERENCES

Adrian, R. H. (1978). Charge movement in the membrane of striated muscle. *Annual Review of Biophysics and Bioengineering* **7**, 85–112.

Adrian, R. H. & Almers, W. (1974). Membrane capacity measurements on frog skeletal muscle in media of low ionic content. *Journal of Physiology* **237**, 573–605.

Adrian, R. H. & Almers, W. (1976). Charge movement in the membrane of striated muscle. *Journal of Physiology* **254**, 339–360.

Adrian, R. H. & Peres, A. (1979). Charge movement and membrane capacity in frog skeletal muscle. *Journal of Physiology* **289**, 83–97.

Chandler, W. K. & Hui, C. S. (1990). Membrane capacitance in frog cut twitch fibers mounted in a double vaseline-gap chamber. *Journal of General Physiology* **96**, 225–256.

Chandler, W. K., Jong, D. S. & Pape, P. C. (1992). Measurement of sarcoplasmic reticulum calcium release in frog cut muscle fibers with EGTA and phenol red. *Biophysical Journal* **61**, A130.

Chandler, W. K., Rakowski, R. F. & Schneider, M. F. (1976). A non-linear voltage-dependent charge movement in frog skeletal muscle. *Journal of Physiology* **254**, 243–283.

Chen, W. & Hui, C. S. (1991). Gluconate suppresses Q_β more effectively than Q_γ in frog twitch fibres. *Biophysical Journal* **59**, 543a.

Csernoch, L., Pizarro, G., Uribe, I., Rodriguez, M. & Rios, E. (1991). Interfering with calcium release suppresses I_γ, the hump component of intramembranous charge movement in skeletal muscle. *Journal of General Physiology* **97**, 845–884.

Garcia, J., Pizarro, G., Rios, E. & Stefani, E. (1991). Effect of the calcium buffer EGTA on the 'hump' component of charge movement in skeletal muscle. *Journal of General Physiology* **97**, 885–896.

Hodgkin, A. L. & Nakajima, S. (1972). The effects of diameter on the electrical constants of frog skeletal muscle fibres. *Journal of Physiology* **221**, 105–120.

Huang, C. L.-H. (1981). Dielectric components of charge movements in skeletal muscle. *Journal of Physiology* **313**, 187–205.

Huang, C. L.-H. (1982). Pharmacological separation of charge movement components in frog skeletal muscle. *Journal of Physiology* **324**, 375–387.

HUANG, C. L.-H. (1983a). Experimental analysis of alternative models of charge movement in frog skeletal muscle. *Journal of Physiology* **336**, 527–543.

HUANG, C. L.-H. (1983b). Time domain spectroscopy of the membrane capacitance in frog skeletal muscle. *Journal of Physiology* **341**, 1–24.

HUANG, C. L.-H. (1986). The differential effects of twitch potentiators on charge movements in frog skeletal muscle. *Journal of Physiology* **380**, 17–33.

HUANG, C. L.-H. (1987). 'Off' tails of intramembrane charge movements in frog skeletal muscle in perchlorate-containing solutions. *Journal of Physiology* **384**, 491–509.

HUANG, C. L.-H. (1990). Voltage-dependent block of charge movement components by nifedipine in frog skeletal muscle. *Journal of General Physiology* **96**, 535–558.

HUANG, C. L.-H. (1991). Separation of intramembrane charging components in low calcium solutions in frog skeletal muscle. *Journal of General Physiology* **98**, 249–264.

HUANG, C. L.-H. & PEACHEY, L. D. (1989). Anatomical distribution of voltage dependent membrane capacitance in frog skeletal muscle fibers. *Journal of General Physiology* **93**, 565–584.

HUANG, C. L.-H. & PEACHEY, L. D. (1992). A reconstruction of charge movement during the action potential in frog skeletal muscle. *Biophysical Journal* **61**, 1133–1146.

HUI, C. S. (1983a). Pharmacological studies of charge movements in frog skeletal muscle. *Journal of Physiology* **337**, 509–529.

HUI, C. S. (1983b). Differential properties of two charge components in frog skeletal muscle. *Journal of Physiology* **337**, 531–552.

HUI, C. S. (1991). Factors affecting the appearance of the hump charge movement in frog cut twitch fibers. *Journal of General Physiology* **98**, 315–347.

HUI, C. S. & CHANDLER, W. K. (1990). Intramembranous charge movement in frog cut twitch fibers mounted in a double vaseline-gap chamber. *Journal of General Physiology* **96**, 257–297.

HUI, C. S. & CHANDLER, W. K. (1991). Q_β and Q_γ components of intramembranous charge movement in frog cut twitch fibers. *Journal of General Physiology* **98**, 429–464.

HUI, C. S. & CHEN, W. (1992a). Separation of Q_β or Q_γ charge components in frog cut twitch fibers with tetracaine. Critical comparison with other methods. *Journal of General Physiology* **99**, 985–1016.

HUI, C. S. & CHEN, W. (1992b). Effects of conditioning depolarization and repetitive stimulation on Q_β and Q_γ charge components in frog cut twitch fibers. *Journal of General Physiology* **99**, 1017–1043.

IRVING, M., MAYLIE, J., SIZTO, N. L. & CHANDLER, W. K. (1987). Intrinsic optical and passive electrical properties of cut frog twitch fibers. *Journal of General Physiology* **89**, 1–40.

IRVING, M., MAYLIE, J., SIZTO, N. L. & CHANDLER, W. K. (1989). Simultaneous monitoring of changes in magnesium and calcium concentrations in frog cut twitch fibers containing antipyrylazo III. *Journal of General Physiology* **93**, 585–608.

MELZER, W., SCHNEIDER, M. F., SIMON, B. J. & SZUCS, G. (1986). Intramembrane charge movement and calcium release in frog skeletal muscle. *Journal of Physiology* **373**, 481–511.

PAPE, P. C., JONG, D. S. & CHANDLER, W. K. (1992). Effects of sarcoplasmic reticulum calcium loading on intramembranous charge movement in frog cut muscle fibers. *Biophysical Journal* **61**, A130.

PIZARRO, G., CSERNOCH, L., URIBE, I., RODRIGUEZ, M. & RIOS, E. (1991). The relationship between Q_γ and Ca release from the sarcoplasmic reticulum in skeletal muscle. *Journal of General Physiology* **97**, 913–947.

SCHNEIDER, M. F. & CHANDLER, W. K. (1973). Voltage-dependent charge in skeletal muscle: a possible step in excitation–contraction coupling. *Nature* **242**, 244–246.

SZUCS, G., CSERNOCH, L., MAGYAR, J. & KOVACS, L. (1991). Contraction threshold and the 'hump' component of charge movement in frog skeletal muscle. *Journal of General Physiology* **97**, 897–911.

VERGARA, J. & CAPUTO, C. (1982). Effects of tetracaine on charge movements and calcium signals in frog skeletal muscle fibers. *Proceedings of the National Academy of Sciences of the USA* **80**, 1477–1481.

Acknowledgements

The author thanks W. Smith for skilled assistance and Anthea Hills for preparation of the manuscript.

Received 22 December 1992; accepted 14 June 1993.